

1 **Shotgun metagenomics reveals an enrichment of potentially cross-reactive bacterial epitopes in**
2 **ankylosing spondylitis patients, as well as the effects of TNFi therapy and the host's genotype upon**
3 **microbiome composition.**

4

5 Jian Yin^{1*}, Peter R. Sternes^{2*}, Mingbang Wang³, Mark Morrison⁴, Jing Song¹, Ting Li¹, Ling Zhou¹, Xin Wu¹,
6 Fusheng He⁵, Jian Zhu⁶, Matthew A. Brown^{2,9}, Huji Xu^{1,6,7⁹}.

7

8 1. Department of Rheumatology and Immunology, Shanghai Changzheng Hospital, Second Military Medical
9 University, Shanghai, China.

10 2. Translational Genomics Group, Institute of Health and Biomedical Innovation, Queensland University of
11 Technology, Translational Research Institute, Brisbane, Australia.

12 3. Shanghai Key Laboratory of Birth Defects, Division of Neonatology, Children's Hospital of Fudan University,
13 National Center for Children's Health, Shanghai, 201102, China.

14 4. University of Queensland Diamantina Institute, Faculty of Medicine, Translational Research Institute, Brisbane,
15 Australia.

16 5. Immunobio, Shenzhen, Guangdong, 518001, China.

17 6. Beijing Tsinghua Changgung Hospital, School of Clinical Medicine, Tsinghua University, Beijing 100084, China.

18 7. Peking-Tsinghua Center for Life Sciences, Tsinghua University, Beijing 100084, China.

19

20 *These authors contributed equally to this manuscript.

21 ⁹ These authors contributed equally to this manuscript.

22

23 Corresponding Author:
24 Professor Matthew A. Brown,
25 Institute of Health and Biomedical Innovation,
26 Queensland University of Technology,
27 Translational Research Institute,
28 Princess Alexandra Hospital,
29 Woolloongabba, Brisbane,
30 Australia.
31 matt.brown@qut.edu.au

32 **ABSTRACT**

33 Diverse evidence including clinical, genetic and microbiome studies support a major role of the gut
34 microbiome in the common immune-mediated arthropathy, ankylosing spondylitis (AS). To further
35 investigate this we performed metagenomic analysis of a case-control cohort of 250 Han-Chinese
36 subjects. Previous reports of gut dysbiosis in AS were re-confirmed and several notable bacterial species
37 and functional categories were differentially abundant. TNF-inhibitor (TNFi) therapy at least partially
38 restored the perturbed microbiome observed in untreated AS cases to that of healthy controls, including
39 several important bacterial species that have been previously associated with AS and other related
40 diseases. Enrichment of bacterial peptides homologous to HLA-B27-presented epitopes was observed in
41 the stools of AS patients, suggesting that either HLA-B27 fails to clear these or that they are involved in
42 driving HLA-B27-associated immune reactions. TNFi therapy of AS patients was also associated with a
43 reduction of potentially arthritogenic bacterial peptides, relative to untreated patients. An AS-associated
44 SNP in *RUNX3* significantly influenced the microbiome in two independent cohorts, highlighting a host
45 genotype (other than *HLA-B27*) potentially influencing AS via the microbiome. These findings emphasise
46 the key role that the gut microbiome plays in driving the pathogenesis of AS.

47 INTRODUCTION

48 Ankylosing spondylitis (AS) is a chronic inflammatory disease affecting primarily the spine and pelvis,
49 causing pain and initially reversible stiffness, and ultimately leading to joint ankylosis due to ectopic
50 bone formation. In a subset of patients, peripheral joints and extra articular tissues including the eye,
51 gut and skin are also involved. Its prevalence in Asian and European descent populations ranges from
52 0.09% to 0.55%^{1,2}, whereas the disease is rare in most of Africa, likely due to the low frequency of the
53 main susceptibility gene, *HLA-B27*³. There is a significant unmet therapeutic need in AS, with limited
54 evidence that current therapies prevent spinal ankylosis, no oral treatments which suppress disease
55 activity other than corticosteroids, and no treatments which have been demonstrated to induce
56 remission or prevent the disease.

57

58 AS has been shown in both twin and unrelated case/control studies to be highly heritable (twins >90%
59 heritability^{4,5}, unrelated case/control common variant heritability 69%
60 (<http://www.nealelab.is/blog/2017/9/15/heritability-of-2000-traits-and-disorders-in-the-uk-biobank>)).

61 Over past decade, at least 116 susceptibility genes have been identified, contributing 29% of the overall
62 risk of the disease⁶. There is substantial evidence suggesting that the interaction between host genetics
63 and gut microbiome is a key driver of the pathogenesis of AS. The high disease heritability indicates that
64 the environmental factors involved in the disease are likely to be ubiquitous. Reactive arthritis is a
65 spondyloarthritis sharing many clinical and genetic features with AS, and is known to be caused by
66 bacterial infections of the gut or urinary tract; a subset of reactive arthritis patients go on to develop AS.
67 About 60% AS patients suffered from subclinical bowel inflammation and 10% of them can be diagnosed
68 as inflammatory bowel disease (IBD)⁷. There is considerable overlap in the overall heritability of AS and
69 IBD⁸, the two diseases are often co-familial⁹, and many shared genetic associations have been
70 identified¹⁰. A bioinformatic study showed that AS susceptibility genes specifically enriched in gut cells

71 are also enriched in ‘response to bacterium’ GO term pathway, and that AS-associated genetic loci are
72 found disproportionately to lie within epigenetic marks of gene activity in gut tissue and cells ¹¹.
73 Germ-free *HLA-B27*-transgenic rats and SKG mice are disease-free ^{12,13}. Studies using sequencing-
74 based bacterial profiling of terminal ileal biopsies showed that AS patients have a distinct microbiome ¹⁴,
75 a finding that has subsequently been reproduced studying stool samples in AS patients and patients with
76 spondyloarthritis (SpA), a broader clinical classification ^{15,16}. There has also been suggestive evidence
77 reported that the gut microbiome is associated with differences in AS disease activity ¹⁷. In addition, one
78 study compared SpA patients’ stool samples before and three months after TNF-inhibitor (TNFi)
79 treatment onset ¹⁸. Although modest changes were found in microbiome alpha-diversity measures after
80 TNFi treatment, no changes in specific bacterial taxa were observed. This may have been related to
81 power or sampling issues, noting that 15/18 patients studied met only the ASAS axial spondyloarthritis
82 classification criteria rather than having the more specific diagnosis, AS. In summation, the above
83 evidence supports the contention that AS status is influenced by interactions between the gut
84 microbiome and the host immune system.

85

86 To date, the mechanisms involved in the interaction between the host immune system and intestinal
87 microbes remain unclear. One hypothesis suggests that HLA-B27 presents specific peptides to CD8+ T
88 cells, leading to pathogenic adaptive immune responses (the ‘arthritogenic peptide theory’). The gut
89 microbiota produce a huge variety and number of peptides, and as such, microbial peptides intrinsic to
90 dysbiosis may activate CD8+ T-cells In that context, Purcell and colleagues identified 7500 such peptides
91 that bind the eight most common *HLA-B27* subtypes ¹⁹. Here, we present our findings from a shotgun
92 metagenomics sequencing study undertaken with stool samples collected from in 250 Chinese
93 individuals, to investigate evidence of dysbiosis in AS, the effect of host genetic makeup and of TNFi

- 94 treatment on the gut microbiota, and to investigate evidence of immunity to HLA-B27 restricted
- 95 microbial peptides in AS cases.

96 **MATERIALS AND METHODS**

97 **Subject recruitment**

98 A total of 127 unrelated Han Chinese AS cases were recruited from the Department of Rheumatology
99 and Immunology of Shanghai Changzheng Hospital (Shanghai, China) from December 2014 to June 2017.
100 All cases met the 1984 modified New York criteria for AS ²⁰. 123 healthy controls (blood donors on no
101 prescription medications) were recruited from Shanghai. All human studies have been approved by the
102 Research Ethical Committee of Second Military Medical University, and all patients and controls gave
103 informed written consent for their participation in the studies. Clinical information was recorded for all
104 patients, including demographic information (gender, age, smoking status and BMI), disease duration,
105 *HLA-B27* carriage, sulfasalazine and TNFi treatment information, the Bath Ankylosing Spondylitis Disease
106 Activity Index (BASDAI) ²¹ and Bath Ankylosing Spondylitis Functional Index (BASFI) ²², and clinical
107 manifestations (inflammatory back pain, uveitis, axial arthritis, peripheral arthritis, ulcerative colitis,
108 Crohns disease, enthesitis, dactylitis and psoriasis). Dietary habits were assessed by a 52-question
109 questionnaire to exclude subjects with special dietary habits such as an entirely plant-based or meat-
110 based diet. Where possible, Student's T test and Fisher's exact test were used to identify differences in
111 the metadata categories between cases and controls.

112

113 **DNA microarray and subject genotyping**

114 Samples were genotyped using the Infinium CoreExome-24v1-1 Chip (Illumina, San Diego, CA, USA)
115 according to the manufacturer's recommendations. Bead intensity data were processed and normalised
116 for each sample, and genotypes called within collection using GenomeStudio.

117

118 SNPs with call rate below 95% or with a Hardy-Weinberg equilibrium of $P < 10^{-6}$ in controls were
119 excluded. For the overlapping SNPs, pairwise missingness tests removed all SNPs with differential

120 missingness ($P < 10^{-7}$). After merging data sets, SNPs with call rate below 98% and samples with call rate
121 below 98% were removed. *HLA* alleles were imputed by SNP2HLA using the Pan-Asian reference panel
122 ^{23,24} and SNPs were extracted by PLINK v.1.90 ²⁵.

123

124 **Shotgun metagenome sequencing**

125 Faecal samples were collected and stored at -80°C prior to DNA extraction. DNA was extracted using a
126 StoolGen DNA kit (CWBiotech Co., Beijing, China). DNA concentrations were determined using a Qubit
127 dsDNA BR assay kit (Thermo Fisher, Foster City, CA, USA). 200 – 500 bp insert size libraries were
128 constructed using a TruSeq DNA Sample Preparation Kit (Illumina, San Diego, CA, USA) and an
129 automated SPRI-Works system (Beckman Coulter, San Jose, CA, USA),

130

131 Quality Control (QC) of each library was carried out using an Agilent 2100 Bioanalyzer (Agilent
132 Technologies, Santa Clara, CA, USA), Qubit dsDNA BR assay kit (Thermo Fisher, Foster City, CA, USA) and
133 a KAPA qPCR MasterMix plus Primer Premix kit (Kapa Biosystems, Woburn, MA, USA) according to the
134 manufacturer's instructions. Libraries that passed QC ($>3 \text{ ng}/\mu\text{L}$) were sequenced using an Illumina
135 HiSeq sequencer (Illumina, San Diego, CA, USA) with the paired-end 150-bp sequencing model based on
136 $>5\text{G}$ raw data output per sample.

137

138 Manual inspection and QC of sequencing reads was conducted using FastQC v10.1 ²⁶. Paired-end reads
139 were joined using PEAR v0.9.10 ²⁷ and adapters were trimmed using Trimmomatic v0.36 ²⁸. Contaminant
140 sequences, such as those mapping to human or PhiX genomes, were filtered using Bowtie2 v2.3.4 ²⁹ and
141 the remaining reads were counted and subsampled to an equal sequencing depth of 3,520,000
142 sequencing reads per sample using SeqTK v1.0 ³⁰. MetaPhlan2 v2.6.0 ³¹ was used for taxonomic
143 classification, PanPhlan v1.2.2 ³² was used for strain-level profiling utilising pre-computed pan-genome

144 references where possible, and HUMAnN2 v0.11.1³³ was used for functional mapping to KEGG
145 Orthogroups (KO) and MetaCyc pathways and utilising a UniRef90 database.

146
147 For prediction of bacterial peptides homologous to previously reported HLA-B27-presented epitopes,
148 bacterial-derived sequencing reads were BLASTXed against a local, BLAST-formatted³⁴, version of the
149 immune epitope database (IEDB) v3.0 (downloaded August 2016)^{35,36}. BLAST best-hits with an E-value <
150 0.1 were retained, annotated according to a published study³⁷ and then counted. The peptides
151 annotated as HLA-B27-presented were compared between AS patients and healthy controls using
152 Fisher's exact test.

153

154 **Statistical Analysis**

155 Abundance tables were arcsine square root transformed prior to analysis. Multidimensional data
156 visualisation was conducted using a sparse partial least squares discriminant analysis (sPLSDA) as
157 implemented in R as part of the MixOmics package v6.3.1³⁸, at the species level using Bray-Curtis
158 distance matrices. Receiver operating characteristic curve was calculated from sPLSDA using the
159 MixOmics package v6.3.1. Controlling for covariates (such as gender, BMI, age and smoking status)
160 where appropriate, multivariate association of the bacterial species composition with metadata of
161 interest was conducted using a PERMANOVA test as part of vegan v2.4-5³⁹. The alpha diversity of
162 bacterial species was calculated using the rarefy function, as implemented in vegan v2.4-5. Univariate
163 association of bacterial species and functional pathways/groups were tested for significance using
164 MaAsLin v0.0.5⁴⁰ and Wilcoxon rank-sum tests as implemented in R⁴¹. Only results which were
165 significant in both tests were reported in the main text. For measurement of microbial epitope richness,
166 the Shannon, Simpson and Chao diversity indices were measured (vegan v2.4-5) and group differences
167 were evaluated using Wilcoxon rank-sum tests. Genetic-relatedness dendrograms for strain-level results

168 from PanPhlAn were calculated using Jaccard distance matrices and hierarchical clustering as
169 implemented in R v.3.5.2.

170

171 **RESULTS**

172 **Gut dysbiosis in ankylosing spondylitis**

173 We initially sought to confirm previous reports of dysbiosis in AS cases. The case and control cohorts
174 were divided into discovery and validation cohorts prior to analysis; the discovery cohort consisted of 97
175 AS cases and 93 healthy controls with age-matched demographics, and the remaining 60 subjects
176 comprised the validation cohort (30 AS cases and 30 healthy controls) (Supplementary Table 1). With
177 the exception of a difference in the mean age in the validation cohorts in which the controls were
178 younger on average than cases, no differences were observed between cases and controls in either the
179 discovery or validation cohorts. PERMANOVA and sPLSDA multivariate analysis revealed significant
180 differentiation between the microbial composition of AS cases and healthy controls for both the
181 discovery ($P = 0.019$) and validation ($P = 0.0006$) cohorts (Figure 1A), consistent with previous reports.
182 Receiver-operator curve analysis showed high discrimination between cases and controls using
183 microbiome data alone (AUC=0.87 in combined discovery and validation cohorts) (Supplementary Figure
184 1).

185

186 Seven bacterial species were identified to be differentially abundant ($P < 0.05$) (i.e. were 'indicator
187 species') between AS cases and healthy controls, in both the discovery and validation cohorts (Figure
188 1B). *Clostridiales bacterium 1 7 47FAA*, *Clostridium bolteae* and *Clostridium hatheway* were found to be
189 enriched in AS cases, whilst *Bifidobacterium adolescentis*, *Coprococcus comes*, *Lachnospiraceae*
190 *bacterium 5 1 63FAA* and *Roseburia inulinivorans* were depleted. Several other differentially abundant
191 species of interest were identified in either the discovery or validation cohort, notably *Prevotella copri*,

192 *Dialister invisus* and *Faecalibacterium prausnitzii*. A full list of differentially abundant taxa in either
193 cohort is available in Supplementary Table 2.

194
195 Six KEGG Orthogroups were also found to be differentially abundant ($P < 0.05$) in both cohorts (Figure
196 1C), however there were no MetaCyc metabolic pathways which were differentially abundant in both
197 cohorts. The commonly-differentiated KEGG Orthogroups were EC 2.6.1.9: histidinol-phosphate
198 transaminase, EC 2.7.4.1: polyphosphate kinase, EC 4.3.3.6: pyridoxal 5'-phosphate synthase, EC
199 1.15.1.1: superoxide proteinase, EC 3.4.21.53: ATP-dependent serine phosphatase, and EC 2.4.2.17: ATP
200 phosphoribosyltransferase. Full lists of the differentially abundant KEGG Orthogroups and MetaCyc
201 metabolic pathways are available in Supplementary Tables 3 and 4, respectively.

202
203 Linear regression was used to investigate the correlation between the indicator species and the
204 commonly-differentiated KEGG Orthogroups. All indicator species, except for *Lachnospiraceae*
205 *bacterium 5 1 63FAA*, were significantly associated ($P < 0.05$) with the KEGG Orthogroups, however the
206 degree of variation explained by these species was typically low with R^2 values ranging from 0.0008 to
207 0.13 (0.043 on average) (Supplementary Table 5).

208
209 Strain-level profiling of the dysbiotic microbes identified in Figure 1B uncovered no discernible
210 differences in strain composition between AS cases and healthy controls, with identical strains often
211 being observed in both case and control subjects. (Supplementary Figure 2). This suggests that gut
212 dysbiosis may primarily be a result of differential abundance at the species level and that functional or
213 metabolic differences in the microbiome occur from common genetic elements amongst the strain
214 population, as evidenced by KEGG Orthogroups being detectable in the majority of samples in Figure 1C.

215

216 **Effect of TNFi therapy upon the microbiome**

217 TNFi treatment is highly effective in AS, and it is feasible that at least some of its benefits occur through
218 effects on the gut microbiome. To test this hypothesis, the discovery and validation cohorts were
219 combined into the following categories: healthy controls (n = 123), AS cases treated with TNFi (either
220 etanercept or infliximab, n = 67), and AS cases who have not received TNFi treatment (n = 60). No
221 statistically significant effect of sulfasalazine treatment was observed (P=0.76, Supplementary Figure 3).
222 Multivariate comparison of TNFi untreated and treated cases revealed an effect of TNFi treatment upon
223 the overall composition of the microbiome (P = 0.022) (Figure 2A). Untreated cases were significantly
224 different to healthy controls (P = 0.0002), whereas treated cases were not significantly different to
225 healthy controls (P = 0.069) indicating that treatment has helped restore the perturbed composition of
226 the microbiome.

227
228 To identify the key species modulated by the effects of TNFi therapy, species which were both (a)
229 perturbed in untreated AS cases relative to healthy controls, and (b) differently abundant in treated
230 cases compared to untreated cases, were first identified (Figure 2B and Supplementary Table 6). Six of
231 the eight identified species exhibited significant depletion in untreated AS cases, however TNFi
232 treatment appeared to restore the abundance of these species to levels indistinguishable from healthy
233 controls. These species were: *Prevotella copri*, *Faecalibacterium prausnitzii*, *Bilophila unclassified*,
234 *Klebsiella pneumoniae*, *Ruminococcus bromii* and *Eubacterium bifforme*. The remaining two species
235 (*Clostridium symbiosum* and *Eggerthella unclassified*) were enriched in untreated AS and their
236 abundance was no longer different to healthy controls in treated cases. The findings in relation to
237 *Prevotella copri* and *Klebsiella pneumoniae* were of particular interest given their previous association
238 with rheumatoid arthritis (RA) and AS, respectively, as was the highly abundant (approximately 20% of
239 total bacterial DNA, on average) *Faecalibacterium prausnitzii* for its notable depletion in several

240 autoimmune diseases⁴². TNFi therapy appeared to partially normalise the dysbiotic bacterial species
241 and KEGG Orthogroups observed in AS cases relative to healthy controls shown in Figures 1B and 1C,
242 however no statistically significant differences between treated and untreated cases were observed,
243 potentially due to sample size constraints (Supplementary Figure 4).

244
245 The above approach was also used to identify metabolic pathways modulated by TNFi therapy. 20
246 MetaCyc metabolic pathways were identified in total and the perturbed abundance observed in
247 untreated AS cases was restored to healthy control levels in 17 of these. In broad terms, these pathways
248 primarily related to amino acid biosynthesis (notably branched-chain and aromatic amino acid
249 biosynthesis), carbohydrate metabolism (notably starch degradation), nucleotide biosynthesis,
250 metabolite biosynthesis and cell structure. Specific details of the 20 differentially abundant MetaCyc
251 pathways are available in Supplementary Table 7.

252
253 Linear regression was used to investigate the association of between the modulated species and
254 modulated pathways (Supplementary Table 8). Except for PWY-6545: Pyrimidine biosynthesis which was
255 not associated with any individual identified species, all the pathways were significantly associated with
256 at least two of the identified species. Similarly, all the species were significantly associated with multiple
257 pathways, however the abundances of *Bilophila unclassified* and *Klebsiella pneumoniae* were inversely
258 correlated with pathway abundance. An increase in *Klebsiella pneumoniae* was associated with a
259 decrease in the abundance of PWY-6737: starch degradation ($P = 0.014$; $R^2 = -0.0426$). The observed
260 decrease in the starch degradation pathway for untreated AS cases is primarily attributed to a depletion
261 of *Faecalibacterium prausnitzii* ($P = 2.38 \times 10^{-24}$; $R^2 = 0.3123$). *Faecalibacterium prausnitzii* also exhibited
262 strong associations with other metabolic pathways.

263

264 Strain-level profiling of the bacterial species outlined in Figure 2B also revealed no discernible
265 differences in strain composition between healthy controls, treated cases and untreated cases,
266 indicating the TNFi therapy affected the relative abundance of each species, not necessarily the
267 underlying strain composition (Supplementary Figure 5).

268

269 **Effect of host genotype upon the microbiome**

270 Genome-wide association studies (GWAS) have identified many genetic loci which are associated with
271 AS. Emerging evidence indicates that alleles such as *HLA-B27* may influence the disease through its
272 effect upon the gut microbiome^{43,44}. To investigate whether additional loci may affect the gut
273 microbiome and potentially influence disease, we performed PERMANOVA analysis upon loci known to
274 be associated with AS.

275

276 Considering non-MHC loci, an association was noted for rs11249215, a SNP in the promoter of runt-
277 related transcription factor 3 (*RUNX3*) gene known to be associated with AS^{45,46}. This variant was
278 associated with a shift in the microbiome of both AS cases and healthy controls (combined $P = 0.0097$).
279 Furthermore, sPLSDA revealed that the degree alteration appears dependent on whether the host
280 carried a heterozygous or homozygous genotype (Figure 3A), with the homozygous genotype resulting in
281 a more substantial shift. As further confirmation, we analysed a recently published 16S metabarcoding
282 dataset⁴⁷ of 107 healthy control subjects which were sampled from six different body sites. This analysis
283 re-confirmed discrimination of the microbiomes based on genotype (PERMANOVA; $P = 0.0001$) (Figure
284 3B). The *RUNX3* SNP had no observable effect upon the dysbiotic bacterial species and KEGG
285 Orthogroups outlined in Figures 1B and 1C, however its effects upon species richness and community
286 composition (Figure 3A) suggest that further research is required to confirm a role in AS pathogenesis
287 via effects upon the microbiome. The effect of *HLA-B27* upon the microbiome of the current cohort was

288 unable to be investigated due to high prevalence of this genotype in AS cases and low prevalence in
289 healthy controls, thus the effect of *HLA-B27* was unable to be discerned from the effect of AS itself.

290

291 To highlight the key bacterial species affected by rs11249215, species associated with the heterozygous
292 (AG) and homozygous (GG) genotypes, or solely the homozygous (GG) genotype were identified (Figure
293 3C). Several bacterial species showed differential abundance for the AG genotype, but not the GG
294 genotype, potentially due to sample size constraints (the GG genotype was present in 37 of the 188
295 genotyped subjects), and thus were excluded from further analysis. Four key species identified as
296 depleted in the AG/GG genotypes were: *Lachnospiraceae bacterium 1 1 57FAA*, *Eubacterium*
297 *ventriosum*, *Citrobacter freundii* and *Citrobacter unclassified* (Supplementary Table 9).

298

299 Six MetaCyc metabolic pathways were found to be differentially abundant when comparing *RUNX3*
300 rs11249215 genotypes (Figure 3D). Similar to the differences found for TNFi therapy, the differential
301 pathways were primarily associated with amino acid and nucleotide biosynthesis, however notable
302 differences in polyamine biosynthesis and pyruvate fermentation (to acetate and lactate) were also
303 observed. Of interest is the polyamine biosynthesis pathway for the role of polyamines in enhancing the
304 integrity of the intestinal epithelial cell barrier, and the adenosine biosynthesis pathway for the anti-
305 inflammatory and immunosuppressant effect of adenosine (Supplementary Table 10)^{48,49}.

306

307 Linear regression of these species with the metabolic pathways revealed relatively marginal
308 associations, with the two *Citrobacter* species exhibiting no association with any metabolic pathway
309 (Supplementary Table 11). 16S rRNA gene metabarcoding analysis of the predominately Caucasian
310 cohort sampled from various body sites (Figure 3B) revealed a different set of taxa and metabolic
311 pathways potentially influenced by the *RUNX3* SNP (Supplementary Tables 12 and 13). The minimal

312 overlap with the current shotgun metagenomic study is potentially indicative of the differences between
313 the metagenomic approaches and/or differences in studied cohorts (i.e. geographic location, diet,
314 ethnicity...etc).

315

316 Similar to the strain-level results for AS status and TNFi therapy, no observable bias in the underlying
317 strain population was observed, indicating that *RUNX3* variants likely affect the relative abundance of
318 species, not necessarily strain composition (Supplementary Figure 6^{47,50}). Comparatively fewer species
319 were associated with the *RUNX3* SNP in comparison to the number of species associated with AS status
320 and TNFi treatment. Consistent with recent publications which have investigated the effect of the host's
321 genotype upon the abundance of specific taxa ^{47,50}, these data provide supporting evidence that the
322 underlying host's genetics may have a generalised effect upon the microbiome, with a subtle effect on a
323 higher number of taxa as opposed to a marked effect on a select few.

324

325 **Bacterial-derived HLA-B27 epitopes in AS cases and healthy controls**

326 The main physiological function of HLA-B27 is to present peptides to CD8 lymphocytes, thereby driving
327 cell mediated immune reactions. Differences in the presence of HLA-B27-positive epitopes in the gut
328 microbiome in cases compared to controls, and in HLA-B27 carriers compared with HLA-B27-negative
329 subjects, would be consistent with effects of HLA-B27 to 'shape' the gut microbiome, and the
330 significance of this in regards disease pathogenesis.

331

332 To investigate the abundance of bacterial peptides homologous to HLA-B27 epitopes in AS cases and
333 healthy controls, translated nucleotide searches were performed against IEBD v3.0, annotated according
334 to a published study ³⁷ and counted. Significant enrichment of these peptide sequences was observed in
335 AS cases, with 24 of these enriched in both the discovery and validation cohorts (Table 1). AS cases not

336 only exhibited enrichment of these peptides but the overall diversity of peptides was increased, with
337 Shannon, Inverse Simpson and Chao diversity indices revealing significant differences between AS cases
338 and healthy controls (Figure 4A).

339

340 TNFi treatment effects were also investigated. The overall abundance and diversity of bacterial peptides
341 homologous to HLA-B27-presented epitopes was significantly different between the different treatment
342 categories (Figure 4B). Untreated AS cases exhibited increased abundance and diversity of peptides. For
343 patients who underwent TNFi therapy, a reduction in these potentially arthritogenic peptides was
344 observed relative to untreated cases, however their levels remained marginally higher than healthy
345 controls.

346 **DISCUSSION**

347 **Gut dysbiosis in ankylosing spondylitis**

348 This study re-confirmed the occurrence of bacterial gut dysbiosis in AS cases and identified seven
349 bacterial species which were commonly differentiated between cases and controls in both the discovery
350 and validation cohorts (Figure 1B). Two of these species, *Bifidobacterium adolescentis* and *Coprococcus*
351 *comes*, have been noted for their depletion in Crohn's Disease⁵¹ and were also observed to be depleted
352 in AS cases in this study. An additional two species previously reported to be associated with AS,
353 *Prevotella copri* and *Dialister invisus*, were found to be differentially abundant in either the discovery or
354 validation cohorts (Supplementary Table 2). In the case of *Prevotella copri*, previous studies have
355 demonstrated enrichment in new onset RA cases yet depletion in chronic RA cases⁵². Consistent with
356 these findings, our study found that *Prevotella copri* was depleted in AS cases within the non-age-
357 matched cohort, for which the demographics were heavily skewed towards older AS patients with long-
358 standing disease (Supplementary Table 1). Previous studies in AS have shown increases in *Prevotellaceae*
359¹⁴, or specifically with this species¹⁵. As discussed below, *Prevotella copri* carriage normalised with TNFi
360 treatment. Further studies will be required to determine if *Prevotella copri* carriage changes with
361 disease duration, as has been reported in RA.

362

363 Carriage of *Dialister* species has been previously associated with disease activity in spondylarthrosis
364 patients¹⁷, but the carriage of *Dialister invisus* has been reported to be decreased in inflammatory
365 bowel disease (IBD)^{53,54}. Whilst we found enrichment of *Dialister invisus* in AS cases in the discovery
366 cohort, this was not confirmed in the validation cohort, nor has it been reported in other AS studies. Its
367 pathogenic significance is therefore uncertain.

368

369 Of particular interest, the notable ‘peace keeping’ microbe *Faecalibacterium prausnitzii* was also found
370 to be depleted in AS cases in the validation cohort. This bacterium has also been consistently shown to
371 be depleted in IBD⁵⁴⁻⁵⁹, and has been previously shown to be depleted in the disease enthesitis-related
372 arthritis, a paediatric disease-classification which includes children with ankylosing spondylitis⁶⁰.
373 *Faecalibacterium prausnitzii* is known to produce butyrate and other metabolites and peptides that have
374 diverse anti-inflammatory effects including promoting T-regulatory cell differentiation⁶¹, influences on
375 Th17 lymphocyte activation, and promotion of gut mucosal barrier function^{59,62,63}. As discussed below,
376 TNFi treatment also led to normalisation of *Faecalibacterium prausnitzii* carriage. These findings suggest
377 that *Faecalibacterium prausnitzii* plays a key anti-inflammatory role in AS, as it does in IBD.

378
379 The power of metagenome sequencing is to augment the widely observed phenomena collectively
380 referred to as “dysbiosis” beyond taxonomy-based assessment of microbiome, and provide a more
381 highly resolved and functional characterisation of the microbiome. Here, variation in several KEGG
382 Orthogroups remained consistent between the discovery and validation cohorts (Figure 1C).
383 Additionally, differential abundance of some MetaCyc metabolic pathways was also observed
384 (Supplementary Table 4), but these differences were not consistent between discovery and validation
385 cohorts; potentially highlighting the confounding influence of the host’s age upon the metabolic
386 composition of the gut microbiome.

387
388 Interestingly, genes encoding pyridoxal 5'-phosphate synthase, an important enzyme for the
389 biosynthesis of vitamin B6, were less abundant amongst the microbiome of AS cases compared to
390 healthy controls in both cohorts. Vitamin B6 plays a role in the maintenance of vitamin homeostasis in
391 colonocytes^{64,65}. It has been found to modulate colonic inflammation and several studies have
392 investigated the role of vitamin B6 for the treatment of inflammation in RA patients⁶⁶⁻⁷¹. Evidence from

393 case-control studies show that RA patients have low vitamin B6 status compared to healthy controls,
394 however intervention studies have yielded inconsistent findings, possibly due to the dose of the
395 administered vitamin B6. The reduced potential for the microbiome of AS patients to produce pyridoxal
396 5'-phosphate synthase, and thus vitamin B6, may warrant further investigation into intervention
397 strategies to mitigate inflammation in AS patients.

398

399 **Effect of TNFi therapy upon the microbiome**

400 Previous study of RA patients before and after synthetic disease-modifying anti-rheumatic drug
401 treatment revealed moderate differences in the gut microbiota composition, with the perturbed
402 microbial composition being partly restored following treatment ⁷². Similarly, analysis of spondylarthrosis
403 patients before and after TNFi therapy also revealed modest differences in microbial composition yet no
404 specific taxon was found to be modulated, likely due to sample size ⁷³. Utilising a larger sample size, we
405 confirmed that TNFi therapy was correlated with a restoration of the perturbed microbial composition,
406 and additionally identified several notable bacterial species modulated by treatment.

407

408 We observed that TNFi therapy restored the depletion of *Faecalibacterium prausnitzii* in AS cases.
409 Restoration of *Faecalibacterium prausnitzii* abundance was also correlated with the restored abundance
410 of aromatic and branched-chain amino acid biosynthesis pathways. A recent ulcerative colitis study ⁵⁵
411 revealed reduced dysbiosis and increased *Faecalibacterium prausnitzii* abundance in responders
412 compared with non-responders following TNFi therapy. Furthermore, recovery of *Faecalibacterium*
413 *prausnitzii* in patients with ulcerative colitis after relapse was associated with maintenance of remission
414 ⁷⁴. Another study demonstrated that treatment of infliximab completely restored *Faecalibacterium*
415 *prausnitzii* concentrations from zero to 1.4×10^{10} bacteria/mL within few days ⁵².

416

417 Another important microbe, *Prevotella copri*, was observed to be enriched to levels closely matched to
418 that of healthy controls following TNFi treatment. Abundance of *Prevotella copri* has previously been
419 shown to be enriched in untreated new onset RA patients yet depleted in chronic RA cases, patients
420 with psoriatic arthritis and healthy controls⁵². Colonisation of SKG mice with *Prevotella copri*-dominated
421 microbiota from RA patients exhibited increased number of Th17 cells in the large intestine⁷⁵. HLA-DR-
422 presented peptides (T cell epitopes) from *Prevotella copri* were recently found to stimulate Th1
423 responses in 42% of new onset RA cases, with subgroups of RA patients demonstrating differential IgG
424 or IgA immune reactivity, providing evidence that *Prevotella copri* is immune-relevant in RA
425 pathogenesis⁷⁶. Additionally, the presence of the *HLA-DRB1* risk allele, which influences disease
426 severity, in RA patients was found to be inversely correlated with *Prevotella copri* abundance^{52,77-79}. A
427 recent study of Chinese AS patients revealed enrichment of *Prevotella copri*, as well as *Prevotella*
428 *melaninogenica* and *Prevotella* sp. C561^{15,80}. Contrasting these results, in the current study we observed
429 depletion of *Prevotella copri* in untreated AS cases, which was restored to the healthy control levels in
430 TNFi-treated patients. These seemingly conflicting reports of *Prevotella copri* abundance may be
431 explained by the large degree of intraspecific genetic diversity of *Prevotella copri* strains, with strain
432 variation adding an additional layer of complexity for predicting the function of *Prevotella copri* in the
433 gut. The *Prevotella* genus also contains members that may be beneficial, and which do not function as
434 pathobionts⁷⁷⁻⁷⁹, with observed enrichment in healthy individuals. Taken together, our results which
435 demonstrate a modulation of *Prevotella copri* abundance in TNFi-treated cases is a noteworthy
436 observation, however without a stronger grasp of the strain-level genome variation within this taxon
437 and their prevalence across our cohort, attempts to therapeutically modulate and predict the effects of
438 *Prevotella copri* remains a significant challenge⁸¹.

439

440 *Klebsiella pneumoniae* has also been suggested to play a significant role in AS pathogenesis⁸², although
441 this remains controversial⁸³. *Klebsiella pneumoniae* notably produces pullulanase, a starch-debranching
442 enzyme which enables the degradation of starch into simple sugars⁸⁴. The apparent arthritogenic
443 effects of dietary starch in AS are based on the concept that the growth of *Klebsiella sp.* are favoured by
444 these diets and drive AS pathogenesis^{85,86}. Consequently, low starch diets have been promoted and are
445 frequently followed by patients⁸⁶, although there is no published evidence to date as to their efficacy in
446 positively affecting AS disease course. Here, we actually observed a depletion of this microbe in
447 untreated cases relative to healthy controls, whereas TNFi-treated cases showed a restoration of this
448 bacterium. Furthermore, our metagenome sequencing data showed an inverse correlation between
449 *Klebsiella pneumoniae* relative abundance and the overall starch degradation metabolic pathway ($P =$
450 0.014 ; $R^2 = -0.043$) (Supplementary Table 5). This pathway not only includes the pullulanase-mediated
451 starch de-branching reaction, but also further downstream reactions including the transport and
452 catabolism of maltodextrins. These findings do not support an association between *Klebsiella*
453 *pneumoniae* and AS pathophysiology, although the role of dietary and/or resistant starches on the gut
454 microbiota and AS warrants further investigation.

455
456 MetaCyc pathway analysis revealed depletion of the aromatic and branched-chain amino acid
457 biosynthesis pathways in untreated AS cases, which are responsible for production of four of the nine
458 essential amino acids in humans (leucine, isoleucine, valine and phenylalanine) (Supplementary Table 7).
459 Vitamin B6 is an essential co-factor for branched-chain amino acid transaminase, the last step of
460 branched-chain amino acid synthesis, and was found to be depleted in RA cases, as previously
461 mentioned. Therefore, in the current study we not only observed a depletion of genes encoding the
462 branched-chain amino acid biosynthesis pathway, but also for the enzyme which synthesises an
463 important co-factor in the process.

464

465 **Enrichment of potentially arthritogenic bacterial peptides**

466 Pathogenic bacteria have long been hypothesised as an immunological triggers of AS pathogenesis. In
467 the current study, patients with AS not only demonstrated an enrichment of bacterial peptides matching
468 HLA-B27 epitopes (Table 1), but the diversity of these peptides was greater overall (Figure 4A). These
469 data provide supporting evidence for the molecular mimicry hypothesis for which bacterial-derived
470 peptides may stimulate AS via cross-activation of autoreactive T- or B- cells, thus leading to
471 autoimmunity. This hypothesis does not however explain the increase in HLA-B27 epitopes amongst AS
472 cases, which could be explained by effects of non-HLA genetic factors, or AS-associated environmental
473 factors. An alternate hypothesis is that their excess carriage is caused by a deficiency in the ability of
474 HLA-B27 to effectively control their presence, consistent with evidence of increased bacterial migration
475 across the gut mucosa in AS ⁸⁷. Interestingly, the modulation of the gut microbiome caused by TNFi
476 treatment restored the elevated abundance and diversity of peptides observed in untreated cases to
477 levels which were more closely matched to healthy controls (Figure 4B). Further research will be
478 required to resolve these alternate hypotheses.

479

480 **Effect of host genotype upon the microbiome**

481 Very recently, it was demonstrated that HLA-B27 is associated with a significant shift in the microbiome
482 in healthy individuals ⁴⁷. Furthermore, in mouse models, MHC polymorphisms were demonstrated to
483 contribute to an individual's microbial composition, thus influencing health ⁸⁸. Our investigation
484 revealed an additional AS-associated SNP, rs11249215 in *RUNX3* ^{45,46}, which was also correlated with a
485 significant shift in bacterial composition (Figure 3A). This result was replicated in a confirmatory dataset
486 of healthy Caucasian individuals (Figure 3B). In addition to potential roles in autoimmune diseases,
487 variants in *RUNX3* have been associated with the intestinal inflammatory disorder celiac disease ⁸⁹, and

488 *RUNX3*-knockout mice spontaneously develop IBD ⁹⁰. It is therefore tempting to hypothesise that the
489 role of *RUNX3* in disease pathogenesis is, at least in part, caused by perturbation of the gut microbiome.
490 Interestingly, subjects homozygous for rs11249215 exhibited a significant decrease in the abundance of
491 the polyamine biosynthesis superpathway (Figure 3D). The intestinal tract contains high levels of
492 polyamines which are critical for cell growth and can stimulate the production of junction proteins
493 which are crucial for regulating paracellular permeability and reinforcing epithelial barrier function.
494 Shifts in host and microbial polyamine metabolism may also alter the cytokine environment and induce
495 cellular processes in both acute and chronic inflammatory settings ⁴⁹. A potential relationship between
496 *RUNX3*, microbial composition, intestinal polyamine levels and epithelial permeability and/or the
497 cytokine environment warrants further investigation.
498

499 **CONCLUSION**

500 In this study we confirm that AS is characterised by gut dysbiosis and identify key indicator species,
501 several of which are shared with IBD. This dysbiosis is associated with functional differences in the
502 microbiome involving known inflammation-related pathways. We demonstrate that treatment with
503 TNFi, which is highly effective in suppressing the clinical manifestations of AS, normalises the gut
504 microbiome, and its functional properties, in AS cases. We further demonstrate that the AS gut
505 microbiome is enriched for bacterial peptides that have previously been shown to be presented by HLA-
506 B27, and that this enrichment is also normalised by TNFi treatment. The impact of the host's genotype
507 upon microbiome composition was also highlighted, with an AS- and IBD-associated SNP in *RUNX3*
508 correlating with a shift in microbiome composition. These findings are consistent with disease models in
509 which AS pathogenesis is driven by interactions between a genetically primed host immune system, and
510 the gut microbiome, and point to potential therapeutic and/or preventative approaches for the disease.

511

512 **AUTHOR CONTRIBUTIONS**

513 Study design was performed by HX, JY and MAB. Subject recruitment and sample collection was
514 performed by JY, JS, TL, LZ, XW and JZ. Metagenomic analysis was performed by PRS, and bacterial
515 epitope studies by JY, FH and MW. The manuscript was prepared by PRS, MM, MAB and HX.

516

517 **ACKNOWLEDGEMENTS**

518 HX is supported by National Science Foundation of China (Grant 81302578) and China Ministry of
519 Science and technology (973 Program of China 2014CB541800). MAB is funded by a National Health and
520 Medical Research Council Senior Principal Research Fellowship (APP1024879).

521

522 REFERENCES

- 523 1. Wang, R. & Ward, M.M. Epidemiology of axial spondyloarthritis: an update. *Current opinion in*
524 *rheumatology* **30**, 137-143 (2018).
- 525 2. Braun, J., *et al.* Prevalence of spondylarthropathies in HLA-B27 positive and negative blood
526 donors. *Arthritis Rheum* **41**, 58-67 (1998).
- 527 3. Brown, M.A., *et al.* Ankylosing spondylitis in West Africans--evidence for a non-HLA-B27
528 protective effect. *Ann Rheum Dis* **56**, 68-70 (1997).
- 529 4. Pedersen, O.B., *et al.* Ankylosing spondylitis in Danish and Norwegian twins: occurrence and the
530 relative importance of genetic vs. environmental effectors in disease causation. *Scand J*
531 *Rheumatol* **37**, 120-126 (2008).
- 532 5. Brown, M.A., *et al.* Susceptibility to ankylosing spondylitis in twins: the role of genes, HLA, and
533 the environment. *Arthritis Rheum* **40**, 1823-1828 (1997).
- 534 6. Ranganathan, V., Gracey, E., Brown, M.A., Inman, R.D. & Haroon, N. Pathogenesis of ankylosing
535 spondylitis - recent advances and future directions. *Nature reviews. Rheumatology* **13**, 359-367
536 (2017).
- 537 7. Mielants, H., *et al.* The evolution of spondyloarthropathies in relation to gut histology. II.
538 Histological aspects. *J Rheumatol* **22**, 2273-2278 (1995).
- 539 8. Ellinghaus, D., *et al.* Analysis of five chronic inflammatory diseases identifies 27 new associations
540 and highlights disease-specific patterns at shared loci. *Nature genetics* **48**, 510-518 (2016).
- 541 9. Thjodleifsson, B., Geirsson, A.J., Bjornsson, S. & Bjarnason, I. A common genetic background for
542 inflammatory bowel disease and ankylosing spondylitis: a genealogic study in Iceland. *Arthritis*
543 *Rheum* **56**, 2633-2639 (2007).
- 544 10. Parkes, M., Cortes, A., van Heel, D.A. & Brown, M.A. Genetic insights into common pathways
545 and complex relationships among immune-mediated diseases. *Nature reviews. Genetics* **14**, 661-
546 673 (2013).
- 547 11. Li, Z., *et al.* Epigenetic and gene expression analysis of ankylosing spondylitis-associated loci
548 implicate immune cells and the gut in the disease pathogenesis. *Genes and immunity* **18**, 135-
549 143 (2017).
- 550 12. Taurog, J.D., *et al.* The germfree state prevents development of gut and joint inflammatory
551 disease in HLA-B27 transgenic rats. *The Journal of experimental medicine* **180**, 2359-2364 (1994).
- 552 13. Rehaume, L.M., *et al.* ZAP-70 genotype disrupts the relationship between microbiota and host,
553 leading to spondyloarthritis and ileitis in SKG mice. *Arthritis & rheumatology* **66**, 2780-2792
554 (2014).
- 555 14. Costello, M.E., *et al.* Brief Report: Intestinal Dysbiosis in Ankylosing Spondylitis. *Arthritis &*
556 *rheumatology* **67**, 686-691 (2015).
- 557 15. Wen, C., *et al.* Quantitative metagenomics reveals unique gut microbiome biomarkers in
558 ankylosing spondylitis. *Genome biology* **18**, 142 (2017).
- 559 16. Breban, M., *et al.* Faecal microbiota study reveals specific dysbiosis in spondyloarthritis. *Ann*
560 *Rheum Dis* **76**, 1614-1622 (2017).
- 561 17. Tito, R.Y., *et al.* Brief Report: Dialister as a Microbial Marker of Disease Activity in
562 Spondyloarthritis. *Arthritis & rheumatology* **69**, 114-121 (2017).
- 563 18. Bazin, T., *et al.* Microbiota Composition May Predict Anti-Tnf Alpha Response in
564 Spondyloarthritis Patients: an Exploratory Study. *Scientific reports* **8**, 5446 (2018).
- 565 19. Schittenhelm, R.B., Sian, T.C., Wilmann, P.G., Dudek, N.L. & Purcell, A.W. Revisiting the
566 arthritogenic peptide theory: quantitative not qualitative changes in the peptide repertoire of
567 HLA-B27 allotypes. *Arthritis & rheumatology* **67**, 702-713 (2015).

- 568 20. Linden, S.V.D., Valkenburg, H.A. & Cats, A. Evaluation of diagnostic criteria for ankylosing
569 spondylitis. *Arthritis & rheumatology* **27**, 361-368 (1984).
- 570 21. Garrett, S., *et al.* A new approach to defining disease status in ankylosing spondylitis: the Bath
571 Ankylosing Spondylitis Disease Activity Index. *J Rheumatol* **21**, 2286-2291 (1994).
- 572 22. Calin, A., *et al.* A new approach to defining functional ability in ankylosing spondylitis: the
573 development of the Bath Ankylosing Spondylitis Functional Index. *J Rheumatol* **21**, 2281-2285
574 (1994).
- 575 23. Das, S., *et al.* Next-generation genotype imputation service and methods. *Nature genetics* **48**,
576 1284 (2016).
- 577 24. Jia, X., *et al.* Imputing amino acid polymorphisms in human leukocyte antigens. *PloS one* **8**,
578 e64683 (2013).
- 579 25. Rentería, M.E., Cortes, A. & Medland, S.E. Using PLINK for genome-wide association studies
580 (GWAS) and data analysis. in *Genome-Wide Association Studies and Genomic Prediction* 193-213
581 (Springer, 2013).
- 582 26. Andrews, S. FastQC: a quality control tool for high throughput sequence data. (2010).
- 583 27. Zhang, J., Kobert, K., Flouri, T. & Stamatakis, A. PEAR: a fast and accurate Illumina Paired-End
584 reAd mergeR. *Bioinformatics* **30**, 614-620 (2013).
- 585 28. Bolger, A.M., Lohse, M. & Usadel, B. Trimmomatic: a flexible trimmer for Illumina sequence
586 data. *Bioinformatics* **30**, 2114-2120 (2014).
- 587 29. Langmead, B. & Salzberg, S.L. Fast gapped-read alignment with Bowtie 2. *Nature methods* **9**, 357
588 (2012).
- 589 30. Li, H. seqtk Toolkit for processing sequences in FASTA/Q formats. (GitHub, 2012).
- 590 31. Truong, D.T., *et al.* MetaPhlan2 for enhanced metagenomic taxonomic profiling. *Nature*
591 *methods* **12**, 902 (2015).
- 592 32. Scholz, M., *et al.* Strain-level microbial epidemiology and population genomics from shotgun
593 metagenomics. *Nature methods* **13**, 435 (2016).
- 594 33. Abubucker, S., *et al.* Metabolic reconstruction for metagenomic data and its application to the
595 human microbiome. *PLoS computational biology* **8**, e1002358 (2012).
- 596 34. Altschul, S.F., Gish, W., Miller, W., Myers, E.W. & Lipman, D.J. Basic local alignment search tool.
597 *Journal of molecular biology* **215**, 403-410 (1990).
- 598 35. Vita, R., *et al.* The immune epitope database (IEDB) 3.0. *Nucleic acids research* **43**, D405-D412
599 (2014).
- 600 36. Kim, Y., *et al.* Immune epitope database analysis resource. *Nucleic acids research* **40**, W525-
601 W530 (2012).
- 602 37. Schittenhelm, R.B., Sian, T.C., Wilmann, P.G., Dudek, N.L. & Purcell, A.W. Revisiting the
603 arthritogenic peptide theory: quantitative not qualitative changes in the peptide repertoire of
604 HLA-B27 allotypes. *Arthritis & rheumatology* **67**, 702-713 (2015).
- 605 38. Lê Cao, K.-A., *et al.* MixMC: a multivariate statistical framework to gain insight into microbial
606 communities. *PloS one* **11**, e0160169 (2016).
- 607 39. Dixon, P. VEGAN, a package of R functions for community ecology. *Journal of Vegetation Science*
608 **14**, 927-930 (2003).
- 609 40. Morgan, X.C., *et al.* Dysfunction of the intestinal microbiome in inflammatory bowel disease and
610 treatment. *Genome biology* **13**, R79 (2012).
- 611 41. Ihaka, R. & Gentleman, R. R: a language for data analysis and graphics. *Journal of computational*
612 *and graphical statistics* **5**, 299-314 (1996).
- 613 42. Forbes, J.D., Van Domselaar, G. & Bernstein, C.N. The gut microbiota in immune-mediated
614 inflammatory diseases. *Frontiers in microbiology* **7**, 1081 (2016).

- 615 43. Kenna, T.J. & Brown, M.A. Immunopathogenesis of ankylosing spondylitis. *Int J Clin Rheumatol* **8**,
616 265-274 (2013).
- 617 44. Rosenbaum, J.T., *et al.* Does the microbiome play a causal role in spondyloarthritis? *Clinical*
618 *rheumatology* **33**, 763-767 (2014).
- 619 45. Evans, D.M., *et al.* Interaction between ERAP1 and HLA-B27 in ankylosing spondylitis implicates
620 peptide handling in the mechanism for HLA-B27 in disease susceptibility. *Nature genetics* **43**,
621 761 (2011).
- 622 46. International Genetics of Ankylosing Spondylitis, C., *et al.* Identification of multiple risk variants
623 for ankylosing spondylitis through high-density genotyping of immune-related loci. *Nature*
624 *genetics* **45**, 730-738 (2013).
- 625 47. Asquith, M., *et al.* HLA alleles associated with risk of ankylosing spondylitis and rheumatoid
626 arthritis influence the gut microbiome. *bioRxiv*, 517813 (2019).
- 627 48. Varani, K., *et al.* The role of adenosine receptors in rheumatoid arthritis. *Autoimmunity reviews*
628 **10**, 61-64 (2010).
- 629 49. Rooks, M.G. & Garrett, W.S. Gut microbiota, metabolites and host immunity. *Nature Reviews*
630 *Immunology* **16**, 341 (2016).
- 631 50. Rothschild, D., *et al.* Environment dominates over host genetics in shaping human gut
632 microbiota. *Nature* **555**, 210 (2018).
- 633 51. Gevers, D., *et al.* The treatment-naive microbiome in new-onset Crohn's disease. *Cell host &*
634 *microbe* **15**, 382-392 (2014).
- 635 52. Scher, J.U., *et al.* Expansion of intestinal *Prevotella copri* correlates with enhanced susceptibility
636 to arthritis. *elife* **2**(2013).
- 637 53. Joossens, M., *et al.* Dysbiosis of the faecal microbiota in patients with Crohn's disease and their
638 unaffected relatives. *Gut* **60**, 631-637 (2011).
- 639 54. Schirmer, M., *et al.* Dynamics of metatranscription in the inflammatory bowel disease gut
640 microbiome. *Nat Microbiol* **3**, 337-346 (2018).
- 641 55. Magnusson, M.K., *et al.* Anti-TNF therapy response in patients with ulcerative colitis is
642 associated with colonic antimicrobial peptide expression and microbiota composition. *Journal of*
643 *Crohn's and Colitis* **10**, 943-952 (2016).
- 644 56. De Preter, V., *et al.* Faecal metabolite profiling identifies medium-chain fatty acids as
645 discriminating compounds in IBD. *Gut*, gutjnl-2013-306423 (2014).
- 646 57. Le Gall, G., *et al.* Metabolomics of fecal extracts detects altered metabolic activity of gut
647 microbiota in ulcerative colitis and irritable bowel syndrome. *Journal of proteome research* **10**,
648 4208-4218 (2011).
- 649 58. Marchesi, J.R., *et al.* Rapid and noninvasive metabonomic characterization of inflammatory
650 bowel disease. *Journal of proteome research* **6**, 546-551 (2007).
- 651 59. Machiels, K., *et al.* A decrease of the butyrate-producing species *Roseburia hominis* and
652 *Faecalibacterium prausnitzii* defines dysbiosis in patients with ulcerative colitis. *Gut* **63**, 1275-
653 1283 (2014).
- 654 60. Stoll, M.L., *et al.* Altered microbiota associated with abnormal humoral immune responses to
655 commensal organisms in enthesitis-related arthritis. *Arthritis Res Ther* **16**, 486 (2014).
- 656 61. Arpaia, N., *et al.* Metabolites produced by commensal bacteria promote peripheral regulatory T-
657 cell generation. *Nature* **504**, 451-455 (2013).
- 658 62. Sokol, H., *et al.* *Faecalibacterium prausnitzii* is an anti-inflammatory commensal bacterium
659 identified by gut microbiota analysis of Crohn disease patients. *Proc Natl Acad Sci U S A* **105**,
660 16731-16736 (2008).
- 661 63. Neis, E., Dejong, C. & Rensen, S.J.N. The role of microbial amino acid metabolism in host
662 metabolism. *7*, 2930-2946 (2015).

- 663 64. Rucker, R.B., Suttie, J.W. & McCormick, D.B. *Handbook of vitamins*, (CRC Press, 2001).
- 664 65. Magnúsdóttir, S., Ravcheev, D., de Crécy-Lagard, V. & Thiele, I. Systematic genome assessment
665 of B-vitamin biosynthesis suggests co-operation among gut microbes. *Frontiers in genetics* **6**,
666 148 (2015).
- 667 66. Woolf, K. & Manore, M.M. Elevated plasma homocysteine and low vitamin B-6 status in
668 nonsupplementing older women with rheumatoid arthritis. *Journal of the American Dietetic*
669 *Association* **108**, 443-453 (2008).
- 670 67. Schumacher, H., Bernhart, F. & György, P. Vitamin B6 levels in rheumatoid arthritis: effect of
671 treatment. *The American journal of clinical nutrition* **28**, 1200-1203 (1975).
- 672 68. Chiang, E.-P.I., Bagley, P.J., Selhub, J., Nadeau, M. & Roubenoff, R. Abnormal vitamin B6 status is
673 associated with severity of symptoms in patients with rheumatoid arthritis. *The American*
674 *journal of medicine* **114**, 283-287 (2003).
- 675 69. Chiang, E.-P.I., Selhub, J., Bagley, P.J., Dallal, G. & Roubenoff, R. Pyridoxine supplementation
676 corrects vitamin B6 deficiency but does not improve inflammation in patients with rheumatoid
677 arthritis. *Arthritis research & therapy* **7**, R1404 (2005).
- 678 70. O'connor, Á. An overview of the role of diet in the treatment of rheumatoid arthritis. *Nutrition*
679 *bulletin* **39**, 74-88 (2014).
- 680 71. Selhub, J., *et al.* Dietary vitamin B6 intake modulates colonic inflammation in the IL10^{-/-} model
681 of inflammatory bowel disease. *The Journal of nutritional biochemistry* **24**, 2138-2143 (2013).
- 682 72. Zhang, X., *et al.* The oral and gut microbiomes are perturbed in rheumatoid arthritis and partly
683 normalized after treatment. *Nature medicine* **21**, 895 (2015).
- 684 73. Bazin, T., *et al.* Microbiota Composition May Predict Anti-Tnf Alpha Response in
685 Spondyloarthritis Patients: an Exploratory Study. *Scientific reports* **8**, 5446 (2018).
- 686 74. Varela, E., *et al.* Colonisation by *Faecalibacterium prausnitzii* and maintenance of clinical
687 remission in patients with ulcerative colitis. *Alimentary pharmacology & therapeutics* **38**, 151-
688 161 (2013).
- 689 75. Maeda, Y., *et al.* Dysbiosis contributes to arthritis development via activation of autoreactive T
690 cells in the intestine. *Arthritis & rheumatology* **68**, 2646-2661 (2016).
- 691 76. Pianta, A., *et al.* Evidence of the immune relevance of *Prevotella copri*, a gut microbe, in patients
692 with rheumatoid arthritis. *Arthritis & rheumatology* **69**, 964-975 (2017).
- 693 77. Glick-Bauer, M. & Yeh, M.-C. The health advantage of a vegan diet: exploring the gut microbiota
694 connection. *Nutrients* **6**, 4822-4838 (2014).
- 695 78. Kovatcheva-Datchary, P., *et al.* Dietary fiber-induced improvement in glucose metabolism is
696 associated with increased abundance of *Prevotella*. *Cell metabolism* **22**, 971-982 (2015).
- 697 79. Kim, D. & Kim, W.U. can *Prevotella copri* be a causative pathobiont in rheumatoid arthritis?
698 *Arthritis & rheumatology* **68**, 2565-2567 (2016).
- 699 80. Wen, C., *et al.* Quantitative metagenomics reveals unique gut microbiome biomarkers in
700 ankylosing spondylitis. *Genome biology* **18**, 142 (2017).
- 701 81. Ley, R.E. Gut microbiota in 2015: *Prevotella* in the gut: choose carefully. *Nature Reviews*
702 *Gastroenterology & Hepatology* **13**, 69-70 (2016).
- 703 82. Ebringer, R., Cooke, D., Cawdell, D.R., Cowling, P. & Ebringer, A. Ankylosing spondylitis: klebsiella
704 and HL-A B27. *Rheumatology and rehabilitation* **16**, 190-196 (1977).
- 705 83. Stone, M., *et al.* Comparative immune responses to candidate arthritogenic bacteria do not
706 confirm a dominant role for *Klebsiella pneumoniae* in the pathogenesis of familial ankylosing
707 spondylitis. *Rheumatology* **43**, 148-155 (2003).
- 708 84. Pugsley, A.P., Chapon, C. & Schwartz, M. Extracellular pullulanase of *Klebsiella pneumoniae* is a
709 lipoprotein. *Journal of bacteriology* **166**, 1083-1088 (1986).

- 710 85. Ebringer, A. & Wilson, C. The use of a low starch diet in the treatment of patients suffering from
711 ankylosing spondylitis. *Clinical rheumatology* **15**, 62-66 (1996).
- 712 86. Rashid, T., Wilson, C. & Ebringer, A. The link between ankylosing spondylitis, Crohn's disease,
713 Klebsiella, and starch consumption. *Clin Dev Immunol* **2013**, 872632 (2013).
- 714 87. Ciccia, F., *et al.* Dysbiosis and zonulin upregulation alter gut epithelial and vascular barriers in
715 patients with ankylosing spondylitis. *Ann Rheum Dis* **76**, 1123-1132 (2017).
- 716 88. Kubinak, J.L., *et al.* MHC variation sculpts individualized microbial communities that control
717 susceptibility to enteric infection. *Nature communications* **6**, 8642 (2015).
- 718 89. Dubois, P.C., *et al.* Multiple common variants for celiac disease influencing immune gene
719 expression. *Nature genetics* **42**, 295-302 (2010).
- 720 90. Brenner, O., *et al.* Loss of Runx3 function in leukocytes is associated with spontaneously
721 developed colitis and gastric mucosal hyperplasia. *Proceedings of the National Academy of*
722 *Sciences of the United States of America* **101**, 16016-16021 (2004).
- 723

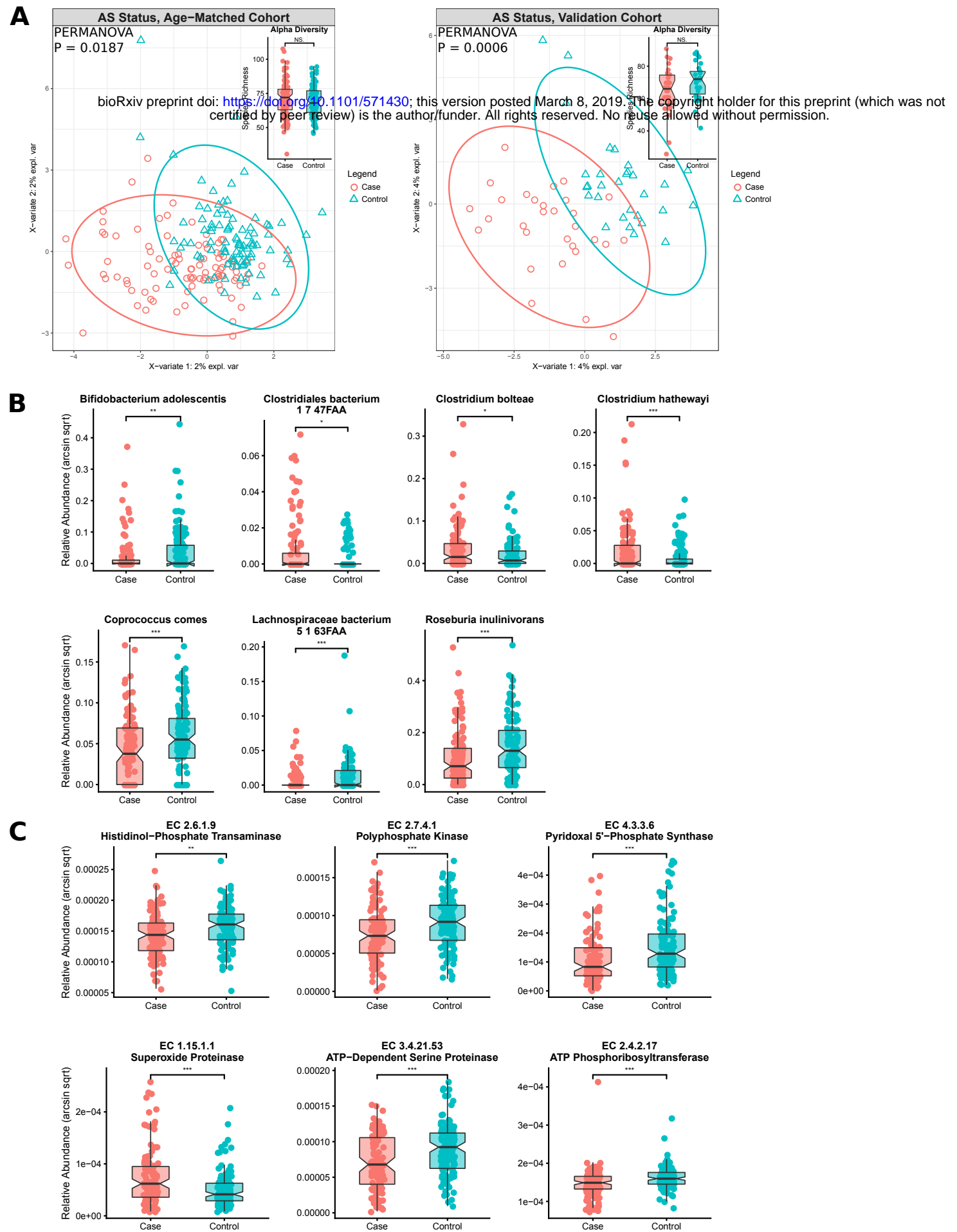


Figure 1: Taxonomic and functional dysbiosis observed in AS cases relative to healthy controls.
A. Alpha and beta diversity analysis. sPLSDA and PERMANOVA revealed community-level differences in taxonomic composition. **B.** Commonly-differentiated bacterial species from the discovery and validation cohorts. **C.** Commonly-differentiated KEGG Orthogroups from the discovery and validation cohorts. Bacterial species and KEGG Orthogroups exhibiting significant results according to multivariate linear modelling and Wilcoxon rank-sum tests are shown.

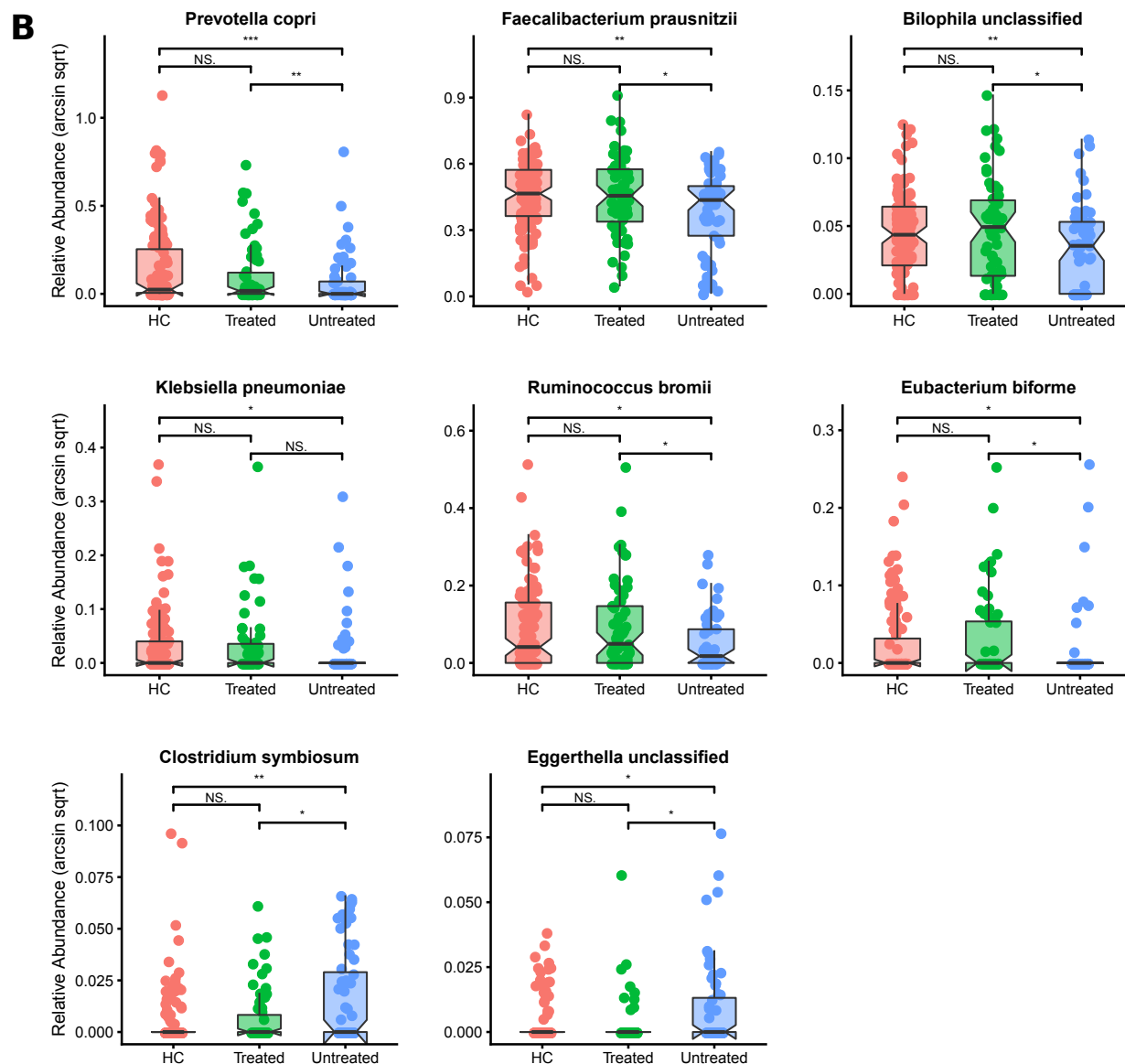
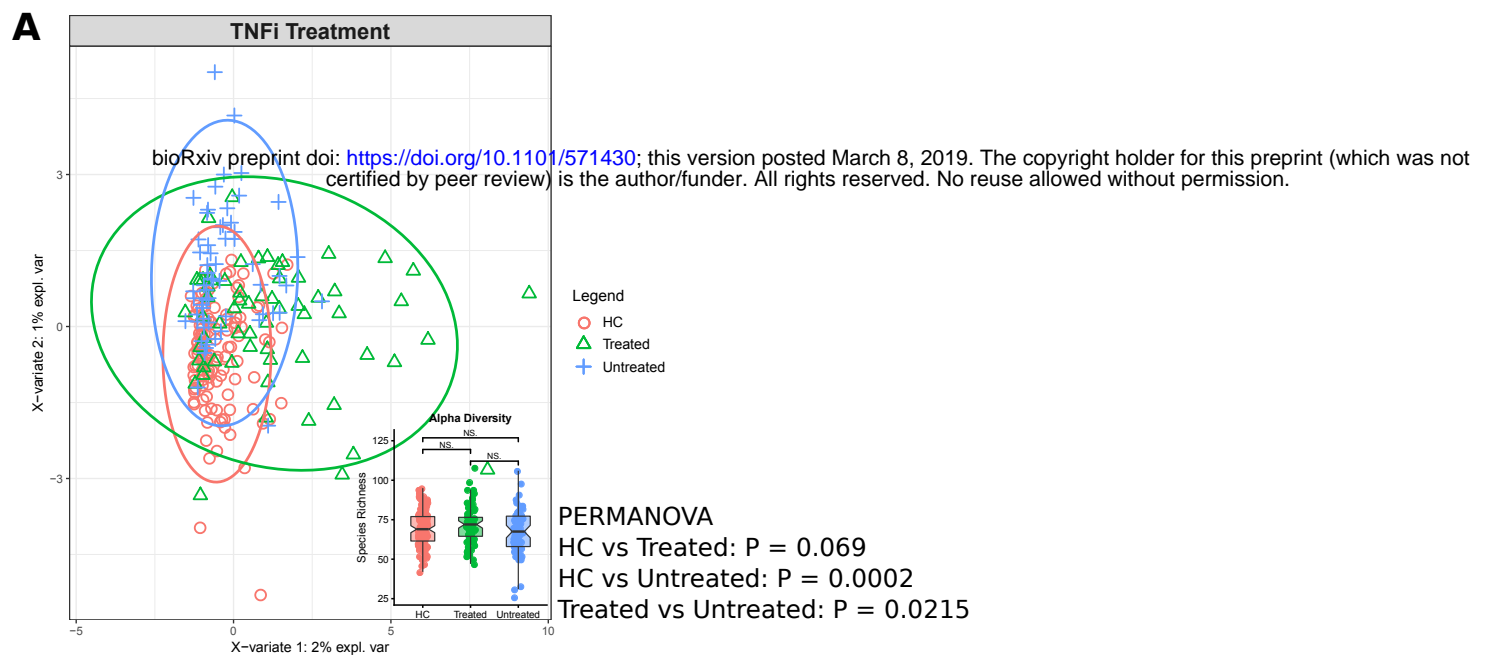


Figure 2: Effect of TNF α therapy upon the microbiome. **A.** Alpha and beta diversity analysis. sPLSDA and PERMANOVA revealed community-level differences in taxonomic composition. **B.** Bacterial species modulated by the effects of TNF α treatment. Bacterial species exhibiting significant results according to multivariate linear modelling and Wilcoxon rank-sum tests are shown.

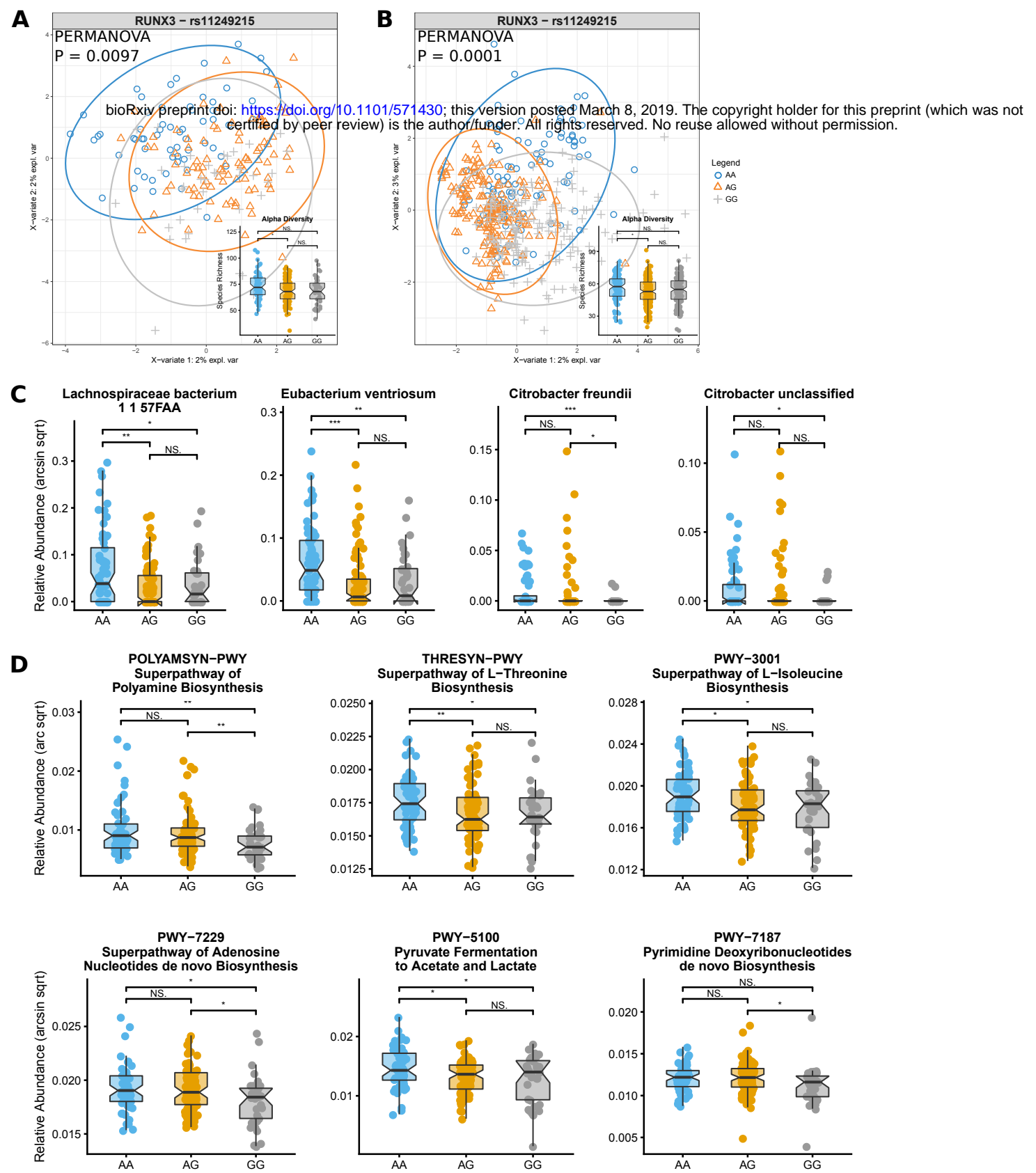


Figure 3: Effect of RUNX3 variants upon the microbiome. **A.** sPLSDA, alpha diversity and PERMANOVA community-level taxonomic analysis of the current study. **B.** sPLSDA, alpha diversity and PERMANOVA community-level taxonomic analysis of a recent 16S metabarcoding study of healthy individuals. **C.** Modulated bacterial species according to significant results from multivariate linear modelling and Wilcoxon rank-sum testing. **D.** Modulated MetaCyc metabolic pathways, according to significant results from multivariate linear modelling and Wilcoxon rank-sum testing.

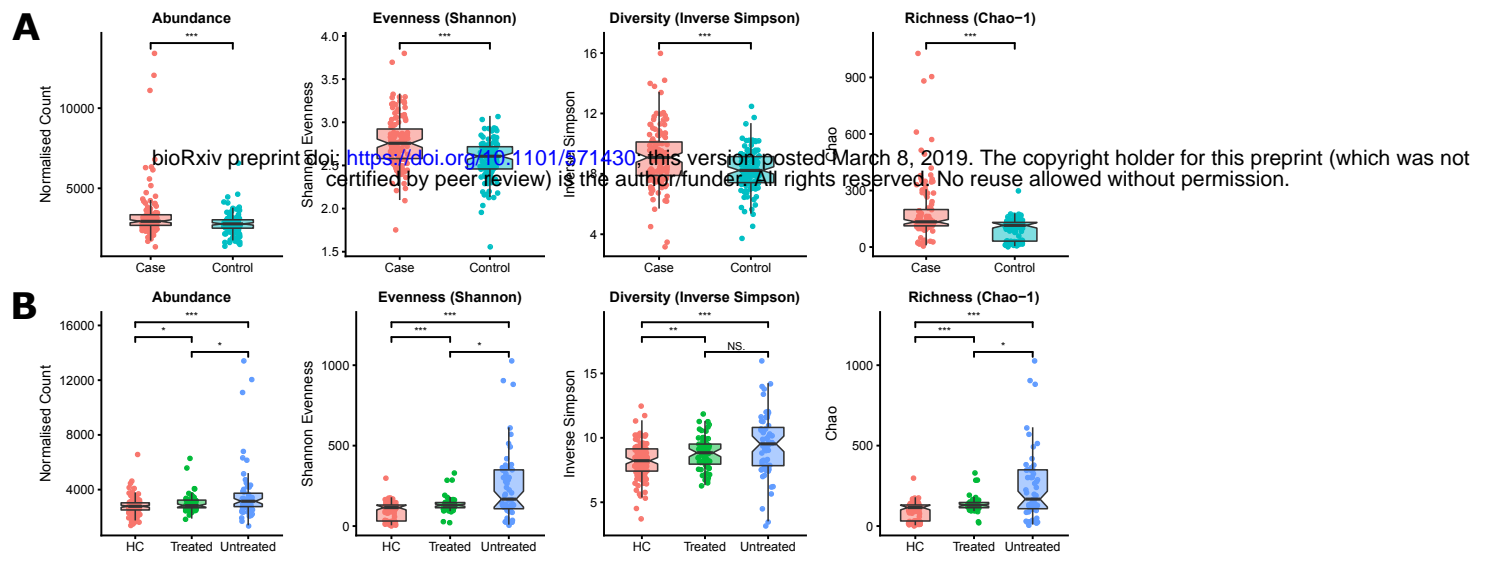


Figure 4: A. Enrichment, both in terms of abundance and diversity, of bacterial peptides homologous to HLA-B27 epitopes in AS cases relative to healthy controls. **B.** Differential abundance and diversity of bacterial peptides homologous to HLA-B27 epitopes in TNFi-treated and –untreated cases, and healthy controls.

Epitope ID	HLA-B27 subtype	Sequence
490238	B2702;B2704	ARFKSNVTKTMKGFY
493378	B2704;B2705;B2709	MRLPAQLLGLLM
493505	B2702	NRHYTFYVW
491582	B2702	GRINPNSGCTNY
494083	B2702	QTTFLVDNKKVFGTHL
494108	B2702	RQIMTGFGEYSY
434944	B2702;B2705;B2707;B2709	ARTPHWALF
492935	B2703	KRWESERVLSF
493023	B2705	LPVNLSTSGPF
492689	B2703;B2707;B2709	KRFDDKYTLKLT
492876	B2702	KRNEDESPNKLY
442808	B2702;B2703;B2708	ARLDIDPETITW
494092	B2702	RKFQPYKPFYY
495095	B2708	SRLEQGEEPWWL
490897	B2702	ERIAEFNQLQF
493564	B2702	NRQIVSGSRDKTIKLW
445935	B2702;B2703;B2707;B2708;B2709	KRNTFVGTPFWM
491482	B2702;B2703;B2704;B2705;B2706;B2707;B2708	GRFTIKSDVWSF
490741	B2702	ATTAALLLEAQAATGFLVDPVR
492710	B2703	KRFFFDVGSNKY
494342	B2707;B2709	RRIMRPTDVPDQGL
447192	B2702	QRGLWGGEW
492970	B2702	KRYDEVEAEGY
493651	B2702	QRAIQVDPNYAY
491073	B2702	FQWMSSRVSPNTLW
494077	B2705	QRYSLLPFWY

Table 1: Bacterial peptides homologous to HLA-B27-presented epitopes which were commonly enriched in the discovery and validation cohorts for AS cases.

bioRxiv preprint doi: <https://doi.org/10.1101/571430>; this version posted March 8, 2019. The copyright holder for this preprint (which was not certified by peer review) is the author/funder. All rights reserved. No reuse allowed without permission.